Supplementary Materials for

Ezh2 Orchestrates Topographic Migration and Connectivity of Mouse Precerebellar Neurons

Thomas Di Meglio, Claudius F. Kratochwil, Nathalie Vilain, Alberto Loche, Antonio Vitobello, Keisuke Yonehara, Steven M. Hrycaj, Botond Roska, Antoine H. F. M. Peters, Anne Eichmann, Deneen Wellik, Sebastien Ducret, Filippo M. Rijli*

Materials and Methods

Generation of Hoxa5::Cre BAC line

The BAC clone RP23-20F21 (BACPAC Resources Center at Children's Hospital Oakland Research Institute, Oakland, Calif., USA) containing the entire *Hoxa* cluster was used as a template for bacterial recombination as described previously (*18*). The plasmid pN21-Cre was used to amplify a Cre-SV40polyA-Frt-Kanamycin-Frt cassette with 70-mer primers containing 50 nucleotides of homology (indicated as caps) surrounding the coding sequence of the *Hoxa5* first exon, such that *Cre* is inserted in-frame with the *Hoxa5* ATG codon. Forward primer: 5'ACGCACAAACGACCGCGAGCCACAAATCAAGCACACATATCAAAAAACAA atgtccaatttactgaccgt3'; reverse primer:, 5'CAAGACCCGCGCCCCCACGGACGCGTGGATCAGAAAACGGCTGGCTTTACt attccagaagtagtgagga3'. To obtain the *Hoxa5::Cre* BAC construct, EL250 bacteria containing the BAC RP23-20F21 were induced for recombination at 42°C and then electroporated with the Cre-SV40polyA-Frt-Kanamycin-Frt cassette. Bacteria were subsequently arabinose-induced for *Flpe* expression in order to remove the kanamycin cassette. Correct recombination and removal of the resistance gene in the *Hoxa5::Cre* BAC were tested by PCR, restriction enzyme digestion and sequencing. Before microinjection, the modified BAC was linearized by PI-SceI digestion. One founder was obtained that displayed the expected *Cre* expression pattern.

Generation of the MafB::CreERT2 line and tamoxifen treatment

The same approach as above was taken using the BAC clone BAC clone RP23-33A18 (BACPAC Resources Center at Children's Hospital Oakland Research Institute, Oakland, CA). The plasmid pN21-CreERT2 was used to amplify a CreERT2-SV40polyA-Frt-Kanamycin-Frt cassette by using 70-mer primers containing 50 nucleotides of homology (indicated as caps) surrounding the coding sequence of the *MafB* gene, such that the Cre is inserted in-frame with the *MafB* ATG codon.

Forward primer:

5'GGCCGCAAAGTTTTCCCCGCGGCAGCGGCGGCTGAGCCTCGCTTTTAGCGA TGtccaatttactgaccgt3';

reverse primer:

5'GAATAGGGAGTCTGGGCCAGGGCAAGGGCGGGGGCCGGACCCGCCAGGAC ctattccagaagtagtgagga3'.

Tamoxifen was dissolved in corn oil and administered by oral gavage at E7.5 (1mg; 100µl of 10mg/ml stock solution).

Generation of r5post::Cre, r5-6::Cre and r7post::Cre lines

We generated transgenic mice in which *Cre* is driven by rhombomere-specific enhancers of *Hoxb3* (*19*) (*r5-post::Cre*), *Hoxa3* (*20*) (*r5-6::Cre*), or *Hoxb4* (*21*) (*r7post::Cre*) (figs. S3 and S4), which were mated to Gt(ROSA)26Sor (*R26R*)^{lacZ} (*22*), *R26R*^{tdTomato} (*23*), or *R26R*^{ZsGreen} (*23*) reporter lines.

The mouse lines were created by replacing the LacZ gene of the pKS-ß-globin-lacZ vector (BGZ40) (*24*) with a Cre cassette (Clontech) using homologous recombination. Enhancers for *Hoxb3* (*19*) (*r5-post::Cre*, 483 bp), *Hoxa3* (*20*) (*r5-6::Cre*, 629 bp) and

Hoxb4 (*21*) (*r7-post::Cre*, 400 bp) were amplified by PCR from genomic DNA using the following primers: *r5-post::Cre:* forward, 5`ATATCCGCGGGATCGGAGAGGAGAGGGCAA; reverse, 5` CGCGACTAGTGATCTCCAAGGTCCCCTTTCA. *r5-6::Cre:* forward, 5`ATATCCGCGGCAACTTGAAAGGGAAGAGCC; reverse, 5` CGCGACTAGTGATATCAAATAGCAGCGAATCTTC. *r7-post::Cre:* forward, 5`ATATCCGCGGTCCTTGGAAGGTATGAATAG; reverse, 5` CGCGACTAGTTGTTACCTCTGAGCCTCTTG. The PCR bands were purified and inserted 5` of the ß-globin promoter using restriction sites FslI and XhoI (*r5-6::Cre*) and BglI and PvuII (*r5-post::Cre, r7-post::Cre*), thus generating constructs consisting of an enhancer, a ß-globin minimal promoter and Cre recombinase encoding sequence. The constructs were linearized, purified and microinjected into the pronuclei of blastocyst embryos. Founders were identified by PCR and screened at P0 after crossing with $R26R^{lacZ}$ animals. 72 animals were genotyped (19 for *r5post::Cre*; 38 for *r5-6::Cre*; 15 for *r7post::Cre*). 19 were positive for Cre (8 for *r5post::Cre*; 8 for *r5-6::Cre*; 3 for *r7post::Cre*). 3/8 showed the expected recombination pattern at P0 for *r5post::Cre*; 2/8 for *r5-6::Cre* and 1/3 for *r7post::Cre*, while the other founders showed no, ubiquitous or ectopic patterns of recombination.

Generation of Hoxa2::Cre line

For the generation of the *Hoxa2::Cre* transgenic line a 3.5kb EcoRI fragment upstream to the *Hoxa2* promoter (from -3585 to -1) was obtained from the plasmid p314R (*25*) and subcloned in a native orientation upstream to a β-globin minimal promoter, the Cre gene and a SV40 polyA signal. The transgene fragment was excised by digestion with SalI and

NotI, and purified before microinjection.

Generation of the ROSA::(lox-STOP-lox)Hoxa2-IRES-EGFP mouse line

The conditional Hoxa2 overexpression mouse line was generated by using the Gateway-compatible *ROSA26* locus targeting vector as previously described (*26*). LR reactions were performed between the plasmid pENTR-FLAG-Hoxa2 (containing the Hoxa2 cDNA coding sequence with a 5'FLAG tag) and the destination vector pROSA26-DV1 to obtain the targeting vector pROSA26-FLAG-Hoxa2-IRES-EGFP. This vector was linearized with PvuI and electroporated into the E14 ES cell line. The positive ES cell clones, selected by G418 resistance and screened by PCR, were aggregated with morula-stage embryos obtained from inbred (C57BL/6 x DBA/2) F1 mice. Germline transmission of the *ROSA26::(lox-STOP-lox)Hoxa2-IRES-EGFP* allele was obtained. Heterozygous and homozygous mice were viable and fertile.

Other mouse lines used in the study

Wnt1::Cre (*27*), *R26R*^{lacZ} (*22*), *Ezh2*$^{fl/fl}$ (kind gift from S.H. Orkin) (*28*), *Hoxa5, Hoxb5, Hoxc5* knockout mice (*29*), *Unc5b*$^{bGal/bGal}$ knockout mice (kind gift from M. Tessier-Lavigne) (*14*) and *Unc5c*^{rcm} (embryos kindly obtained from V. Castellani) (*30*) were as described. *Pcp2::Cre* (*31*), *R26R*^{tdTomato}, *R26R*^{ZsGreen} (*23*) and *Shh*^{tm2Amc} (Shh^{fl}) mice (*32*) were obtained from Jackson Laboratory.

Circuit tracing

G-deleted rabies virus vectors encoding mCherry (SADΔG-mCherry) or eGFP (SADΔG-eGFP) were harvested from BHK-B19G cells (kind gift from E. Callaway) and centrifuged as described previously (*33*). Stereotaxic injections of viruses to different

areas of neocortex or cerebellum were performed via pulled-glass pipettes using a microinjector (Narishige, IM-9B). Pups were anesthetized by hypothermia, injected at P2 and perfused at P7.

In utero electroporation

In utero electroporation was performed on embryos at E13.5 or E14.5 as described previously (*34*) using different combinations of *eGFP* (pCX-eGFP (*35*)), *Unc5b* (pcDNA- *ratUnc5b* (*36*)), *Unc5c* (pcDNA 3.1-*mouseUnc5c*; kind gift from P. Mehlen) and *Netrin1* (pcDNA 3.1-*humanNetrin1*; kind gift from P. Mehlen) expressing vectors diluted to 1 mg/ml in 1x phosphate buffer (PBS1x). Electroporated brains between E16.5 and P0 were fixed for 30 min in paraformaldehyde (PFA, Merck) 4%/ PBS1x. For rescue experiments on *r5-6::Cre;Ezh2*$^{fl/fl}$ embryos, the proportions of ectopic neurons were quantified by Imaris (Bitplane). A Student's t-test was used for statistical analysis.

Histological analysis, immunostaining, and *in situ* hybridization

Prenatal or postnatal brains, dissected when necessary, were fixed in 4% PFA diluted in phosphate buffer (PBS 1x) from 30 minutes to overnight. For cryostat sections, tissues were cryoprotected in 10% sucrose (Fluka) / PBS1x and embedded in gelatine 7.5% (Sigma) / 10% sucrose / PBS1x before being frozen at -80°C. Cryostat sections (20 µm and 30 µm) were cut (Microm HM560) in coronal and sagittal orientations, respectively. Vibratome sections (80 µm or 35 µm for reconstruction) were prepared from postnatal brains after embedding in 4% agarose (Promega)/0.1 M phosphate buffer (pH 7.4). Immunohistochemistry was performed as described in (*6, 29*) using rabbit anti-mouse

Pax6 (Millipore; AB2237; 1/1000^{em}), anti-Hoxa5 antibody (Sigma; HPA029319; 1/200^{em}), rat anti-mouse Hoxb4 (developed by A. Gould and R. Krumlauf; obtained from the Developmental Studies Hybridoma Bank developed under the auspices of the NICHD and maintained by The University of Iowa, Department of Biology, Iowa City, IA 52242; 1/100^{em}) or rabbit anti-mouse trimethyl-histone H3 Lys27 (07-449; Millipore; 1/250^{em}), followed by species-specific fluorochrome-coupled secondary antibody staining, including donkey anti-rabbit A546 (Invitrogen; 1/1000^{em}) and the donkey anti-rat A488 (Invitrogen; 1/1000^{em}) diluted in solutions containing DAPI (Invitrogen). Simple and double *in situ* hybridizations were performed as described previously(*6*). The following probes were used: *Barhl1; Hoxa2; Hoxb3; Hoxb4; Hoxb5, Hoxa5* (*6, 29*), *Ntn1* (*6, 11*), *Unc5b and Unc5c* (*37*). X-galactosidase staining on whole embryos, whole brains or cryostat sections was performed as described in (*6*).

Imaging and Picture Processing

Imaging of fluorescent signals was performed using an Axio imager Z2 upright microscope coupled to a LSM700 Zeiss laser scanning confocal 5x lens (NA 0.25), 10x lens (NA 0.45) or oil/glycerol/water immersion lens 25x (NA 0.8). Stitching of whole-mounts (electroporated brains) was performed using Zen Software at postnatal stages, and using Xuvtools (http://www.xuvtools.org) at prenatal stages. Chromogenic staining was examined by classical wide-field or binocular microscopy (Nikon). Fig. 2I is an inverted artificial superposition of chromogenic signals from adjacent sections. In Fig. 3A, B inverted X-Gal signal is artificially projected onto Pax6 immunohistochemistry.

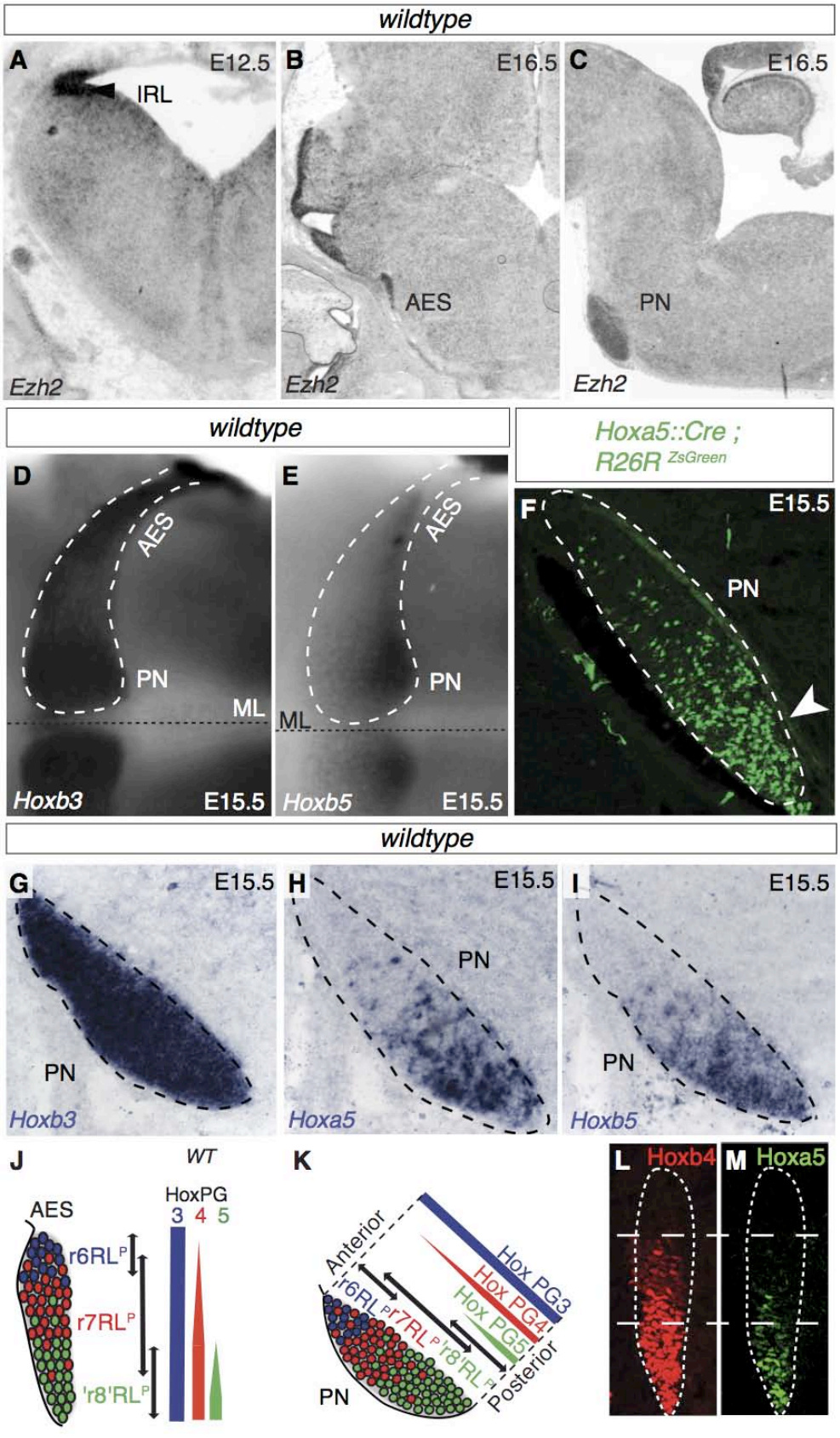
wildtype
A
E12.5
IRL
Ezh2
B
E16.5
AES
Ezh2
C
E16.5
PN
Ezh2
wildtype
Hoxa5::Cre ;
R26R ZsGreen
D
AES
PN
ML
Hoxb3
E15.5
E
AES
PN
ML
Hoxb5
E15.5
F
E15.5
PN
wildtype
G
E15.5
PN
Hoxb3
H
E15.5
PN
Hoxa5
I
E15.5
PN
Hoxb5
J
WT
AES
HoxPG
3 4 5
r6RL^P
r7RL^P
'r8'RL^P
K
Anterior
r6RL^P
r7RL^P
'r8'RL^P
Hox PG3
Hox PG4
Hox PG5
PN
Posterior
L
Hoxb4
M
Hoxa5

Fig. S1. *Ezh2* and *Hox* gene expression in precerebellar rhombic lip derivatives. (A to **C**) *Ezh2 in situ* hybridization on coronal (A, B) and sagittal sections (C). At E12.5 *Ezh2* is expressed in lower rhombic lip (lRL, A) and maintained in E16.5 anterior extramural stream (AES, B) and pontine nuclei (PN, C). (**D** to **E)** E15.5 whole-mount hindbrains show *Hoxb3* expression in all pontine neurons (D) and *Hoxb5* restriction to the posterior PN (E). (**F**) Sagittal section of E15.5 *Hoxa5::Cre;R26R*^{ZsGreen} specimen revealing the localization of ZsGreen^{+} neurons to the posterior PN (arrowhead). **(G** to **I)** E15.5 PN sagittal sections show *Hoxb3* expression in all pontine neurons (G) and restriction of *Hoxa5*$^{+}$ (H) and *Hoxb5*$^{+}$ *(*I) cells to the posterior PN. (**J** to **K**) Summaries of Fig. 2A-I and fig. S1D-I. (**L** to **M**) Hoxb4 (L) and Hoxa5 (M) immunostaining on a coronal section of a E14.5 wildtype embryo. ML: ventral midline.

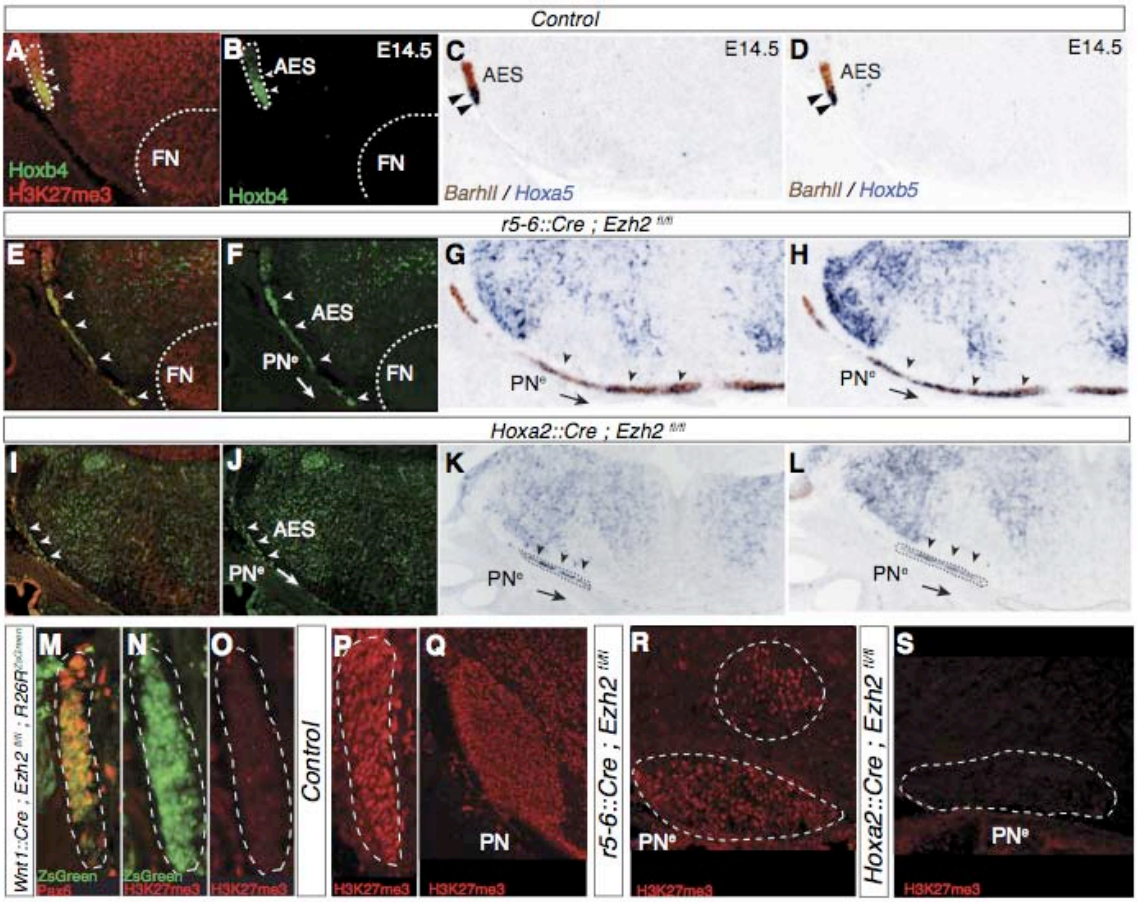

Fig. S2. Hox gene expression in migrating pontine neurons of *Ezh2* conditional mutants. (**A** to **L**) H3K27me3/Hoxb4 immunostaining (A,B,E,F,I,J), *Hoxa5*/*Barhl1* (C,G,K) and *Hoxb5*/*Barhl1* (D,H,L) *in situ* hybridization on coronal sections at r5-r6 level in control (A-D), *r5-6::Cre;Ezh2*$^{fl/fl}$ (E-H) and *Hoxa2::Cre;Ezh2*$^{fl/fl}$ (I-L) E14.5 fetuses. Strong reduction of H3K27me3 in the r5-r6 environment of *Ezh2* conditional knockouts (E,F,I,J). In control (A-D), arrowheads show restricted ventral expression of Hoxb4 (A,B), *Hoxa5* (C) and *Hoxb5* (D) in the anterior extramural stream (AES). In *r5-6::Cre;Ezh2*$^{fl/fl}$ embryos, Hoxb4^{+} pontine neurons migrate to ectopic pontine nuclei (PN^{e}), are Ezh2$^{+/+}$ (co-labeled by H3K27me3/Hoxb4 double immunostaining (arrowheads, E,F)), and express both *Hoxa5* and *Hoxb5* (arrowheads, G,H). In *Hoxa2::Cre;Ezh2*$^{fl/fl}$ embryos, Hoxb4^{+} pontine neurons migrate ectopically to PN^{e} are *Ezh2*$^{-/-}$ as shown by the lack of H3K27me3 (arrowheads, I,J), and express both *Hoxa5* and *Hoxb5* (arrowheads, K,L). The neurons of the facial nucleus (FN), a r4 derivative, still carry the H3K27me3 mark in *r5-6::Cre;Ezh2*$^{fl/fl}$ embryos, showing the specificity of the knockout (E). (**M** to **P**) Pax6 (M) and H3K27me3 (N,O,P) immunohistochemistry of *Wnt1::Cre;Ezh2*$^{fl/fl}$*;R26R*^{ZsGreen} (M-O) and control AES (P) on coronal sections. In the conditional knockout, ZsGreen^{+} pontine neurons express Pax6 (M), but lack the H3K27me3 mark (N,O) in contrast to controls (P). (**Q to S**) H3K27me3 immunohistochemistry on sagittal sections at E18.5 showing loss of the H3K27me3 mark in environment only (R, *r5-6::Cre;Ezh2*$^{fl/fl}$) or environment and PN^{e} (S, *Hoxa2::Cre;Ezh2*$^{fl/fl}$*)* unlike in controls (Q).

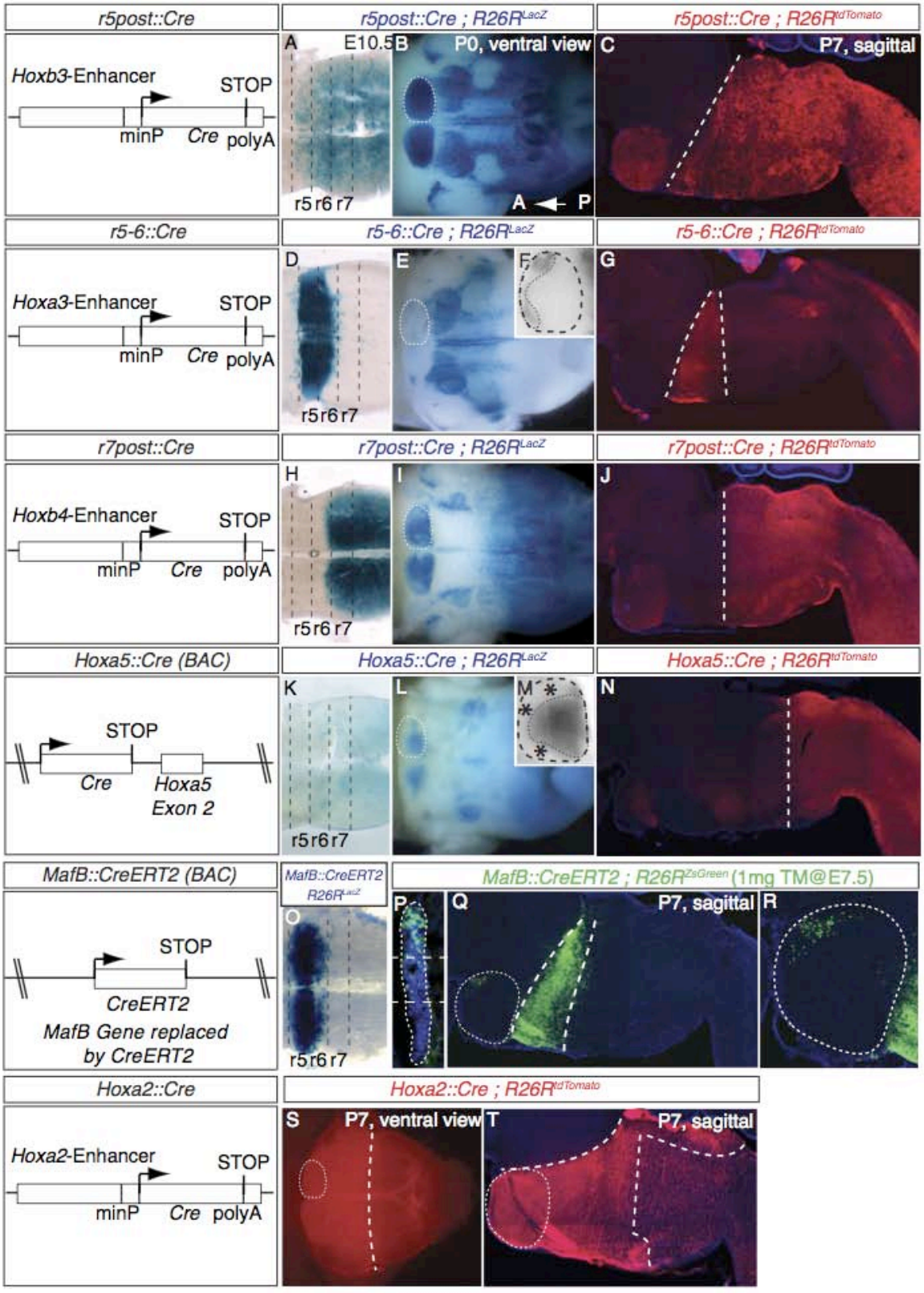

Fig. S3. Generation and characterization of posterior hindbrain Cre-expressing lines. (**A,D,H,K,O***)* Embryos carrying *r5post::Cre* (A), *r5-6::Cre* (D), *r7post::Cre* (H)

and *MafB::CreERT2 (*1mg Tamoxifen@E7.5*)* (O) transgenes crossed to the *R26R*^{lacZ} floxed reporter and expressing *ß-galactosidase* (*ßGal*) at E10.5 in a rhombomere-specific manner, with *r5post::Cre* expression spanning r5 to spinal cord (A), *r5-6::Cre* and *MafB::CreERT2* spanning r5 and r6 (D, O), and *r7post::Cre* spanning r7 to spinal cord (H). *Hoxa5::Cre* is not expressed in the hindbrain before E10.5 (K). (**B,E,I,L,S**) Detection of the *ßGal* on whole-mount hindbrains (ventral views) at P0 show the spatially-restricted progeny of these rhombomeres traced after recombination of the *R26R*^{LacZ} locus in each of these Cre or CreERT2 expressing lines (B,E,I,L) or in (S) using the *R26R* ^{tdTomato} reporter line at P7 for *Hoxa2::Cre*. (**F,M**) High magnifications show the segregation of r6 (*r5-6::Cre*, (F)) (rostrally) and *Hoxa5* (i.e. 'r8') (caudally) progenies (M) in the pontine nuclei. (**C,G,J,N,T**) Sagittal sections at P7 show recombined, *tdTomato*$^{+}$ rhombomere progenies of indicated genotypes; segregation of rhombomere-derived territories persists up to postnatal stages. (**P** to **R**) Coronal (P, E15.5) and sagittal sections (Q,R, P7) of *Mafb::CreERT2; R26R*^{ZsGreen} show the dorsal restriction of r5-6 progeny in the anterior extramural stream (P) and the restriction of ZsGreen^{+} cells to the anterior pontine nuclei (R). r: rhombomere; minP: minimal promoter.

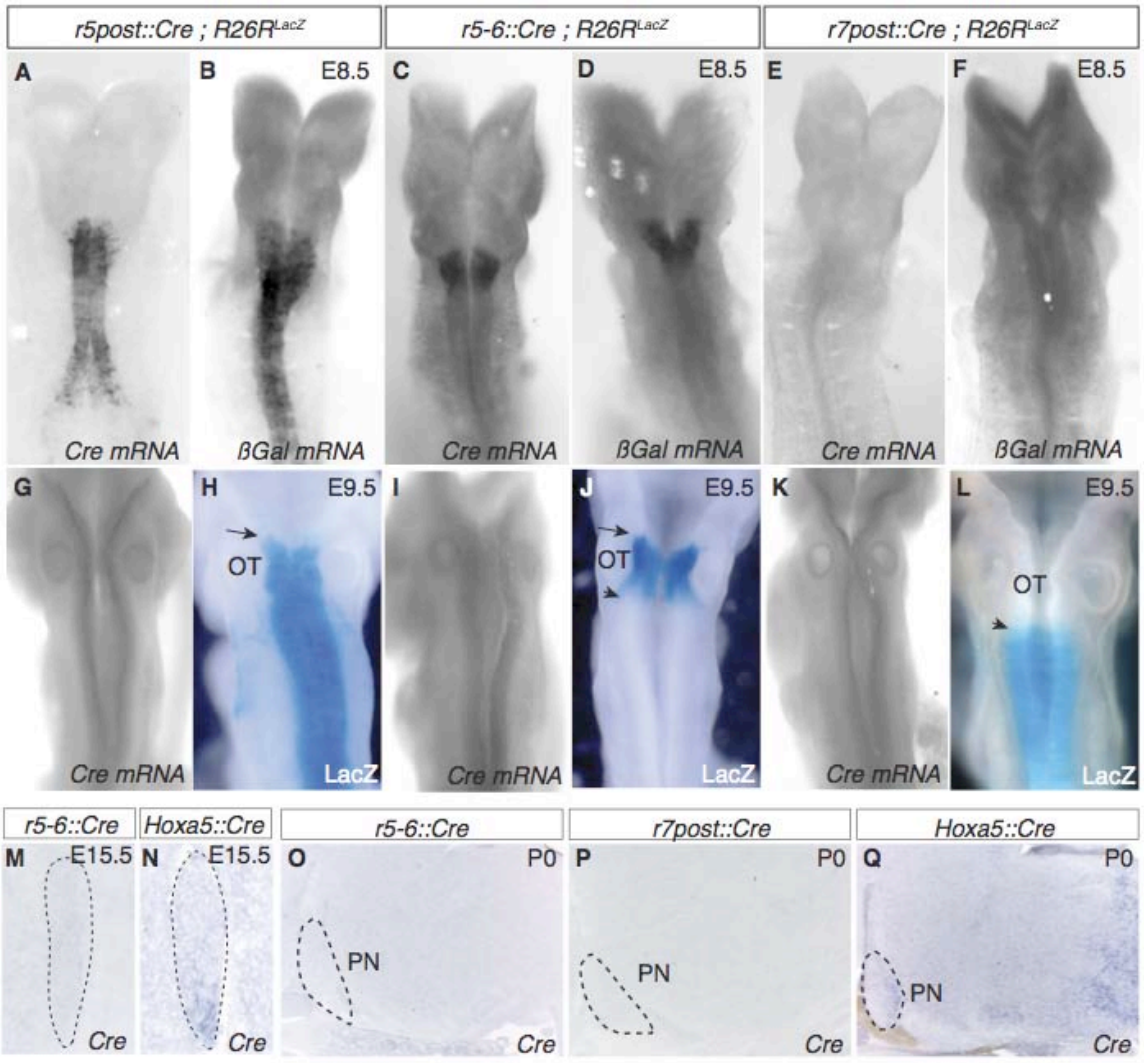

Fig. S4. *Cre* expression patterns in transgenic lines. (**A** to **D**) At E8.5, *Cre* (A,C) and *ß-galactosidase* (*ßGal*) (B,D) are expressed in *r5post::Cre* (A,B) and *r5-6::Cre* (C,D) whole-mount embryos. (**E** to **F**) In *r7post::Cre*, neither *Cre* nor *ß-Gal* are expressed at E8.5. (**G, I, K**) At E9.5, *Cre* transcripts were not detectable in any of the *Cre* transgenics. **(H, J, L**) LacZ signals reveal that the *R26R*^{LacZ} locus has recombined in all three *Cre* transgenics at E9.5. *r5post::Cre* (H) and *r5-6::Cre* (J) share the same *ßGal* anterior boundary (arrow), while *r5-6::Cre* (J) and *r7post::Cre* (L) have their posterior and anterior expression boundaries, respectively, at the r6/r7 border with no overlap (arrowhead). Note that *r7post::Cre;R26R*^{lacZ} show LacZ restricted activity at E9.5 (L), although *Cre* and *ßGal* transcript levels are below *in situ* hybridization detection at E8.5 and E9.5 (E,F,K). (**M** to **N)** *In situ* hybridizations on coronal sections of E15.5 AES show no expression of *Cre* in *r5-6::Cre* (M), while in *Hoxa5::Cre* embryos *Cre* expression faithfully recapitulates endogenous *Hoxa5* expression (N). (**O** to **Q**) On P0 sagittal sections, *Cre* transcripts are not present at detectable levels in *r5-6::Cre* (O) and *r7post::Cre* (P), while *Hoxa5::Cre* newborns show *Cre* expression in posterior hindbrain and posterior PN (Q). OT: otic capsule; PN: pontine nuclei.

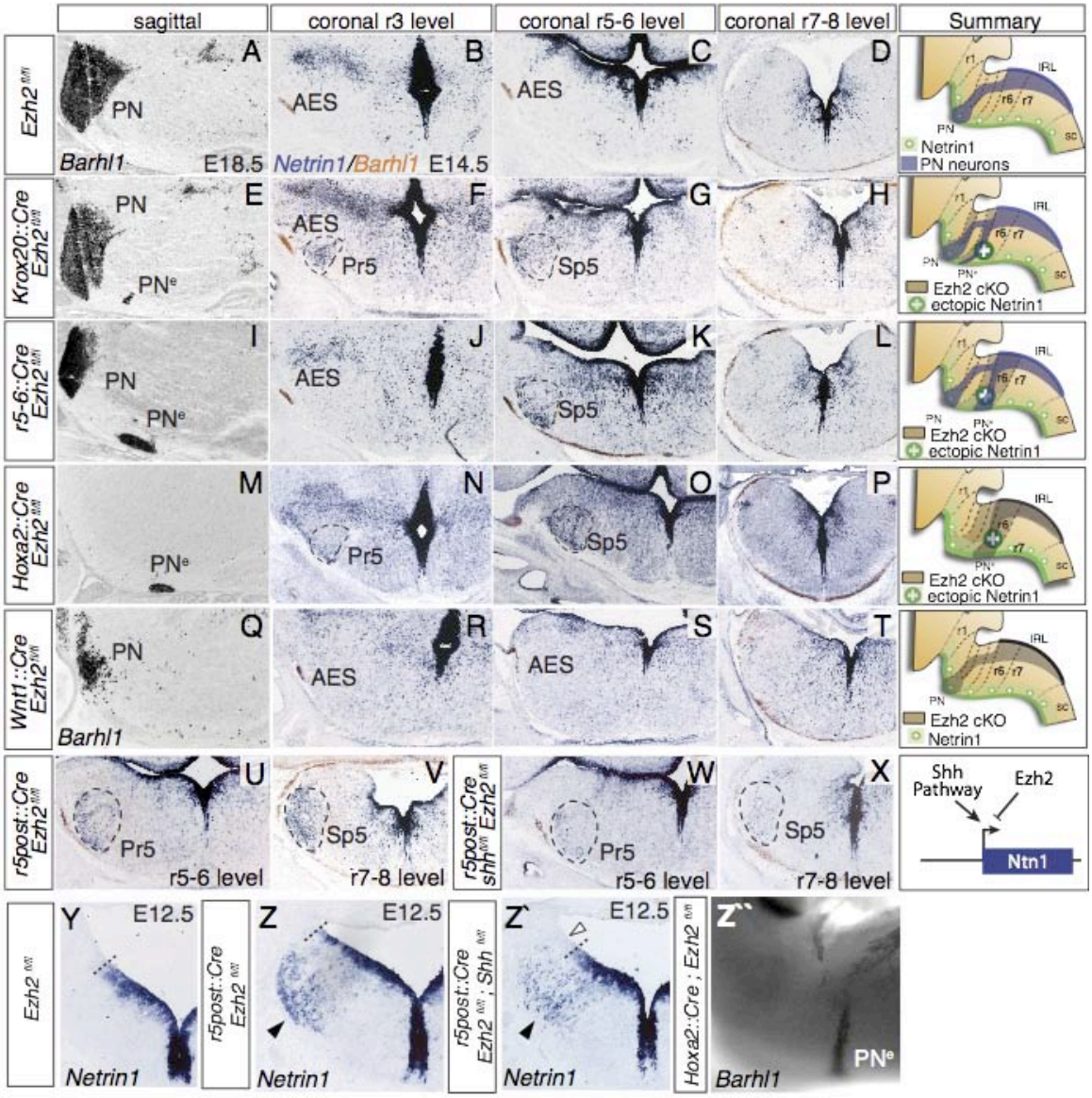

Fig. S5. Analysis of pontine neuron migratory phenotypes in *Ezh2* conditional mutants. (**A** to **T**), PN migratory phenotype in control *Ezh2*$^{fl/fl}$ (A-D), *Krox20::Cre;Ezh2*$^{fl/fl}$ (E-H), *r5-6::Cre;Ezh2*$^{fl/fl}$ (I-L), *Hoxa2::Cre;Ezh2*$^{fl/fl}$ (M-P) and *Wnt1::Cre;Ezh2*$^{fl/fl}$ (Q-T) fetuses. *In situ* hybridization on sagittal sections show rostrocaudal distribution of normal (PN) and ectopic (PN^{e}) *Barhl1*$^{+}$ pontine neurons at E18.5 in the different genotypes (A,E,I,M,Q). Co-detection of *Netrin1* and *Barhl1* transcripts on serial coronal sections taken at the r3, r5/r6 and r7/r8 levels show ectopic expression of *Netrin1* in *Krox20::Cre;Ezh2*$^{fl/fl}$, *r5-6::Cre;Ezh2*$^{fl/fl}$ and *Hoxa2::Cre;Ezh2*$^{fl/fl}$ (dashed lines, F,G,K,N,O) but not in *Wnt1::Cre;Ezh2*$^{fl/fl}$ and *Ezh2*$^{fl/fl}$ embryos at E14.5. (**U** to **X**) Expression of *Netrin1* and *Barhl1* in *r5post::Cre;Ezh2*$^{fl/fl}$ (U, V) and *r5post::Cre;Ezh2*$^{fl/fl}$*;Shh*$^{fl/fl}$ (W,X) at r5/r6 (U, W) and r7/r8 (V, X) levels at E14.5. Ectopic *Netrin1* expression is strongly reduced in *Shh/Ezh2* double cKO (W,X) partially rescuing the *Ezh2* cKO phenotype (U,V). (**Y** to **Z`**) At E12.5, ectopic *Netrin1* expression (black arrowheads) observed in *r5post::Cre;Ezh2*$^{fl/fl}$ mutants (Z) is absent in controls

Ezh2$^{fl/fl}$ (Y) and partially rescued in *r5post::Cre*;*Ezh2*$^{fl/fl}$;*Shh*$^{fl/fl}$ compound mutants (white and black arrowheads, Z`). (**Z``**) Migratory phenotypes in *Hoxa2::Cre;Ezh2*$^{fl/fl}$ shown by *Barhl1 in situ* hybridization on E14.5 whole-mount. Summaries show the migratory pathways of wildtype and mutants as well as the proposed genetic interaction between Shh, Ezh2 and Netrin1 in the last column. AES: anterior extramural stream; lRl: lower rhombic lip; r: rhombomere; sc: spinal cord; Pr5: principal trigeminal nucleus; Sp5: spinal trigeminal nucleus; cKO: conditional knockout.

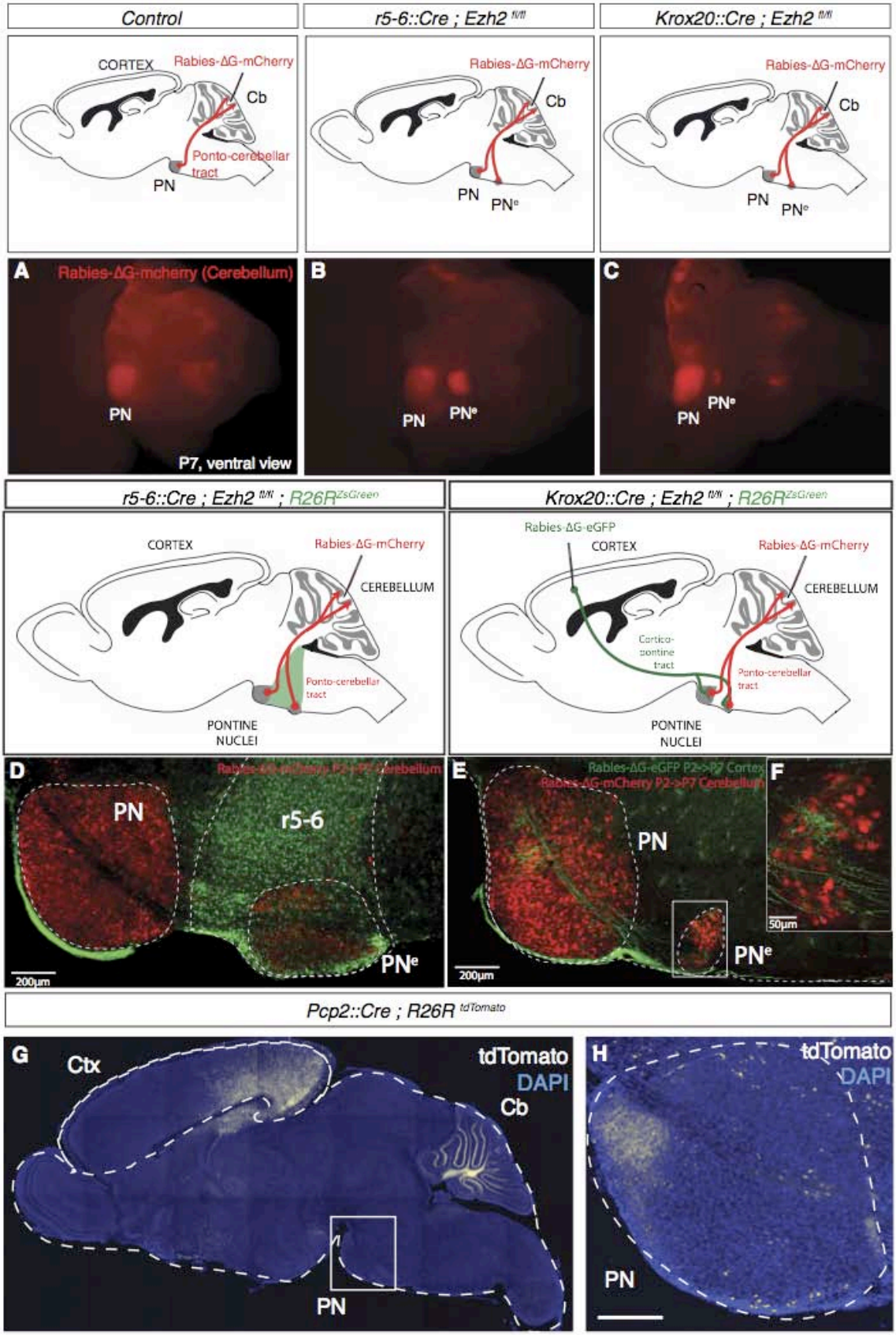
Control
r5-6::Cre ; Ezh2 fl/fl
Krox20::Cre ; Ezh2 fl/fl
CORTEX
Rabies-ΔG-mCherry
Cb
Ponto-cerebellar tract
PN
PNe
A
Rabies-ΔG-mcherry (Cerebellum)
P7, ventral view
B
C
r5-6::Cre ; Ezh2 fl/fl ; R26RZsGreen
Krox20::Cre ; Ezh2 fl/fl ; R26RZsGreen
Rabies-ΔG-eGFP
CEREBELLUM
Cortico-pontine tract
PONTINE NUCLEI
D
r5-6
200µm
E
F
50µm
Pcp2::Cre ; R26R tdTomato
G
Ctx
tdTomato
DAPI
H

Fig. S6. Cortico-ponto-cerebellar connectivity in *Ezh2* conditional mutants. (**A** to **C**) Ventral views of P7 whole-mount hindbrains after retrograde tracing with rabies-ΔG-mCherry from cerebellum (Cb) show that Cb is innervated by normal pontine nuclei (PN) in control (A) and both PN and ectopic pontine nuclei (PN^e) in *Krox20::Cre;Ezh2$^{fl/fl}$* (B) and *r5-6::Cre;Ezh2$^{fl/fl}$* (C) mutants. (**D**) Retrograde injections in P7 *r5-6::Cre;Ezh2$^{fl/fl}$;R26R^{ZsGreen}* animals show that PN^e is included within the $ZsGreen^+$ domain demonstrating PN^e localization in posterior r5/r6 as well as the duplication of both parts of the PN, i.e. reticulotegmental nucleus (inner nucleus) and pontine gray nucleus (outer nucleus). (**E** to **F**) Cortical injections of rabies-ΔG-GFP combined with retrograde cerebellar tracing (rabies-ΔG-mCherry) illustrate that in P7 *Krox20::Cre;Ezh2$^{fl/fl}$* pups, PN^e (F) is also integrated into cortico-ponto-cerebellar connectivity. Injections were carried out at P2 and analyzed at P7. (**G** to **H**) Restricted *tdTomato*$^+$ cells in posterior/visual cortex (Ctx) in P7 *Pcp2::Cre;R26R^{tdTomato}* pups (G) and *tdTomato*$^+$ axon projection to anterior PN in sagittal sections (H).

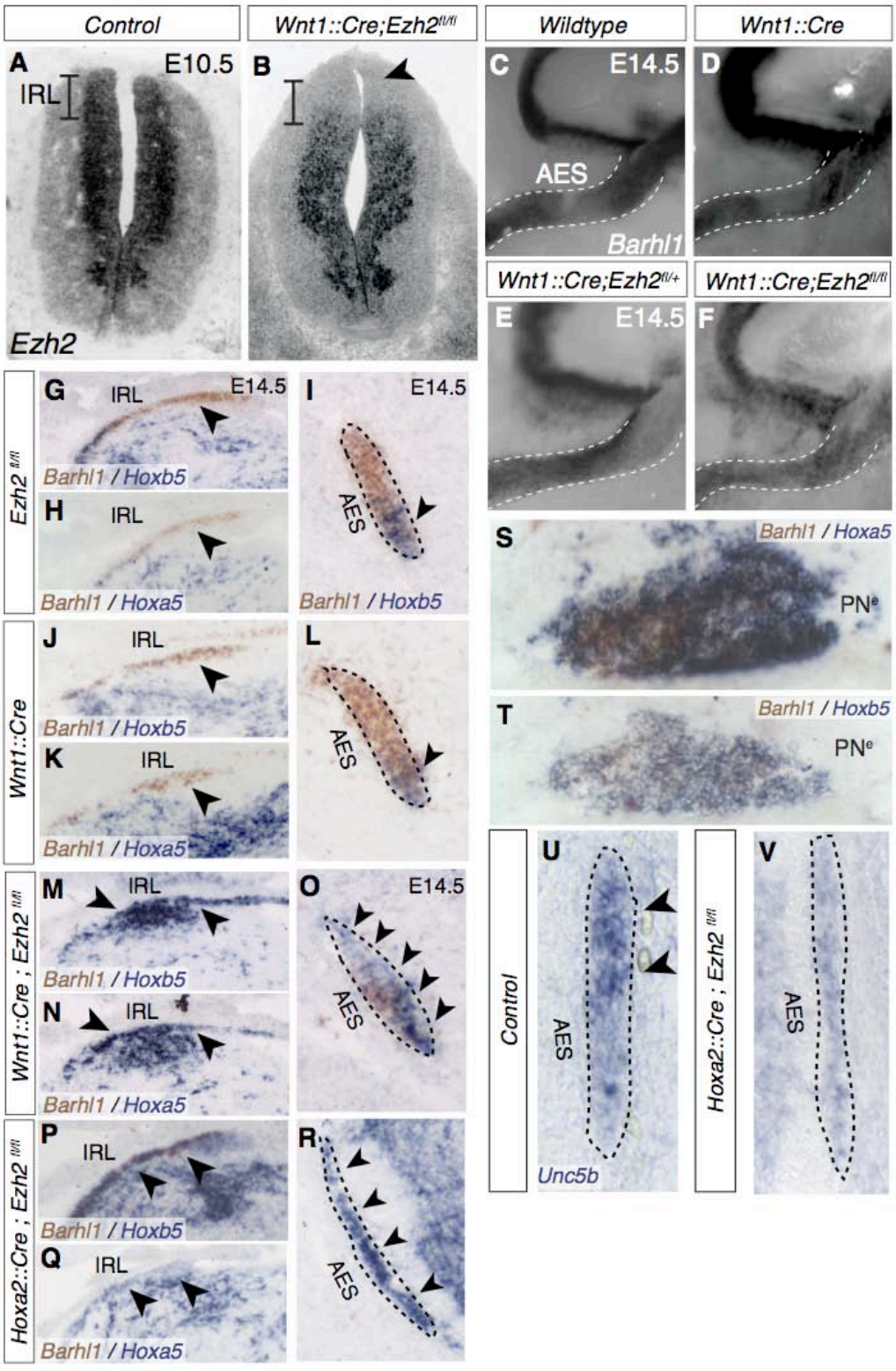

Fig. S7. *Ezh2* cell-autonomous role in rhombic lip and pontine neurons. **(A** to **B)** *Ezh2* is downregulated in the lower rhombic lip (lRL) of *Wnt1::Cre Ezh2*$^{fl/fl}$ embryos at E10.5 (B, arrowhead) compared to controls (A). (**C** to **F**) Lateral views of *Barhl1*$^{+}$

anterior extramural stream (AES) in E14.5 wild type (C), *Wnt1::Cre* (D), *Wnt1::Cre*;*Ezh2*$^{fl/+}$ (E), and *Wnt1::Cre*;*Ezh2*$^{fl/fl}$ (F) conditional mutant whole-mount hindbrains. (**G** to **R**) Co-detection of *Hoxb5* and *Barhl1* (G,I,J,L,M,O,P,R) and *Hoxa5* and *Barhl1* (H,K,N,Q) expression on coronal sections from E14.5 embryos (G-I, *Ezh2fl/fl*; J-L, *Wnt1::Cre*), *Wnt1::Cre:Ezh2*$^{fl/fl}$ (M-O) and *Hoxa2::Cre:Ezh2*$^{fl/fl}$ (P-R) at anterior precerebellar lRL (G,H,J,K,M,N,P,Q) and AES levels (I,L,O,R). In controls *Hoxa5* and *Hoxb5* transcript is absent from the anterior precerebellar lRL (arrowheads, G,H,J,K) and restricted to the ventral AES (I,L). In both *Wnt1::Cre:Ezh2*$^{fl/fl}$ and *Hoxa2::Cre:Ezh2*$^{fl/fl}$ conditional knockouts, *Hoxa5* and *Hoxb5* are expressed ectopically in the anterior precerebellar lRL (arrowheads, M,N,P,Q) and throughout the AES (arrowheads, O,R), while expression is regionalized in controls (arrowheads, H,J). (**S** to **T)** Co-detection of *Hoxa5 (S)*, *Hoxb5 (T)* and *Barhl1 (S,T)* transcripts in E18.5 *Hoxa2::Cre:Ezh2*$^{fl/fl}$ ectopic pontine nuclei (PN^{e}) on sagittal sections. (**U** to **V**) Dorsal *Unc5b* expression at E14.5 in coronal control AES (U), as compared to *Hoxa2::Cre Ezh2*$^{fl/fl}$ AES (V) showing *Unc5b* downregulation. PN: pontine nuclei.

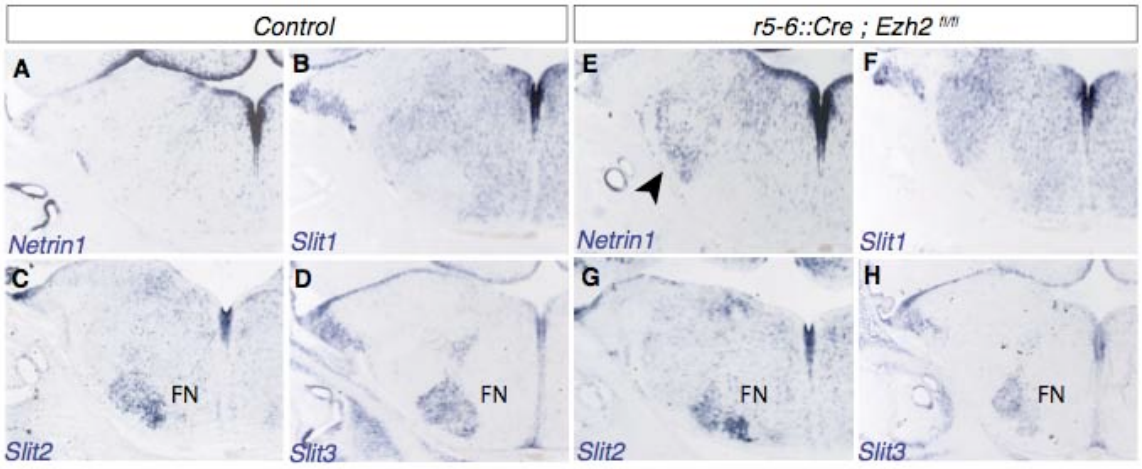

Fig. S8. *Slit1-3* expression patterns in conditional *Ezh2* mutants. (**A** to **H**) *In situ* hybridization for *Netrin1* (A,E), *Slit1* (B,F), *Slit2* (C,G) and *Slit3* (D,H) on adjacent coronal sections at r5-r6 level in E14.5 control (A-D) and *r5-6::Cre;Ezh2*$^{fl/fl}$ (E-H). *Netrin1* is ectopically expressed in *r5-6::Cre;Ezh2*$^{fl/fl}$ (arrowhead, E). FN: facial motor nucleus

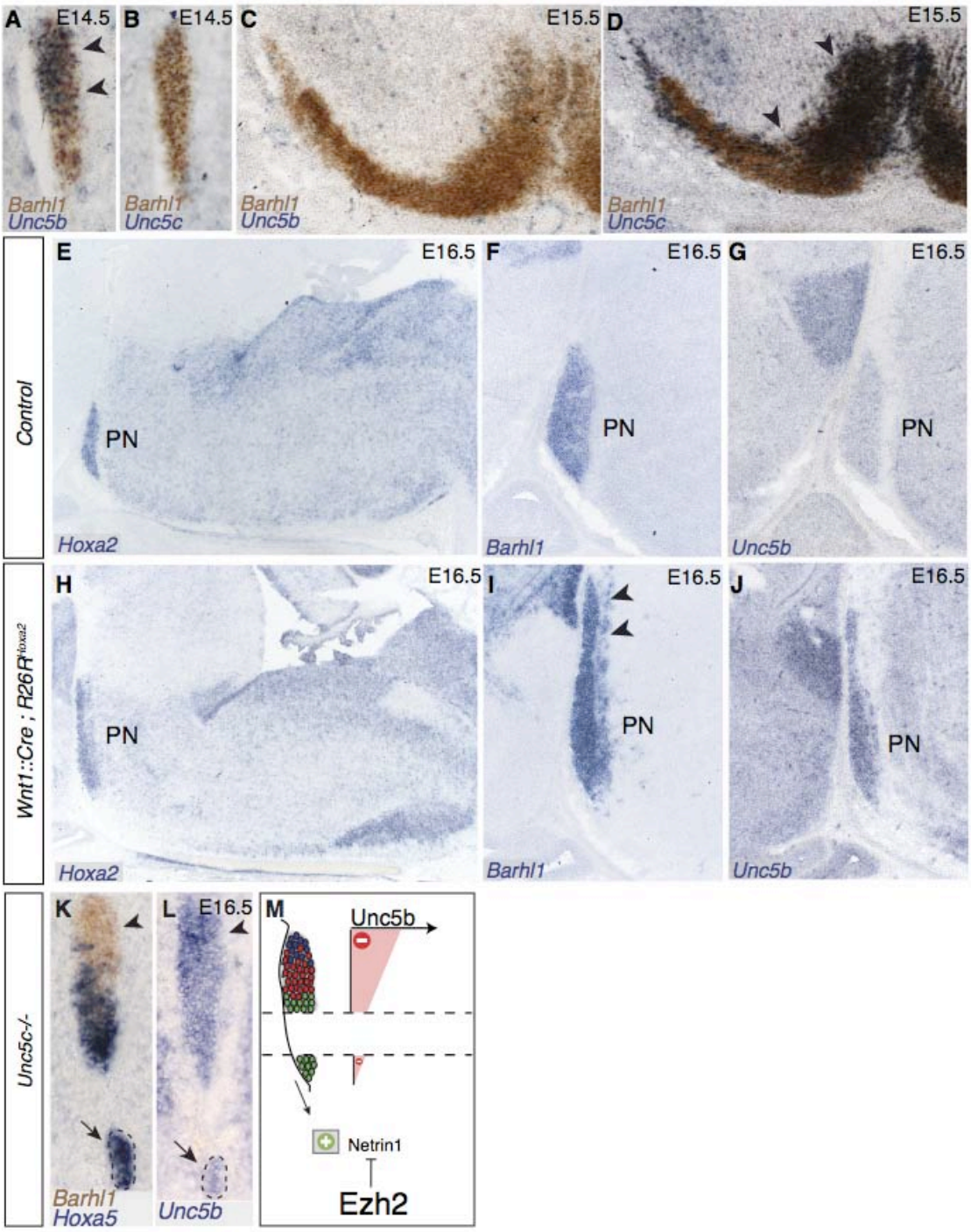

Fig. S9. *Unc5b* and *Unc5c* expression during normal pontine neuron migration and in *Wnt1::Cre;R26R*^{Hoxa2} mutants. (**A** to **D**) Double *in situ* hybridizations for *Barhl1/Unc5b* (A,C) and *Barhl1/Unc5c* (B,D) on coronal sections at E14.5 (A,B) and E15.5 (C,D). *Unc5b* transcripts are detected in the dorsal part of the anterior extramural stream (AES) (arrowheads, A) and become undetectable in *Barhl1*$^{+}$ neurons reaching the ventral midline (C). On the contrary, *Unc5c* transcript expression is undetectable in AES neurons (B) while is reactivated during the second phase of ventral migration

(arrowheads, D). (**E** to **J**) *In situ* hybridization for *Hoxa2* (E,H), *Barhl1* (F,I) and *Unc5b* (G,J) on E16.5 sagittal sections in controls (E-G) and *Wnt1::Cre;R26R*^{Hoxa2} embryos (H-J). In the latter, pontine nuclei (PN) are anteriorly extended (arrow, I) and overexpress *Unc5b* (J), which is undetectable in control E16.5 PN (G). (**K** to **M**) *Hoxa5/Barhl1* (K) and *Unc5b* (L) expression in E16.5 *Unc5c*$^{-/-}$ AES. Ectopically migrating neurons (arrows) strongly express *Hoxa5* while do not express *Unc5b*, as summarized in (M).

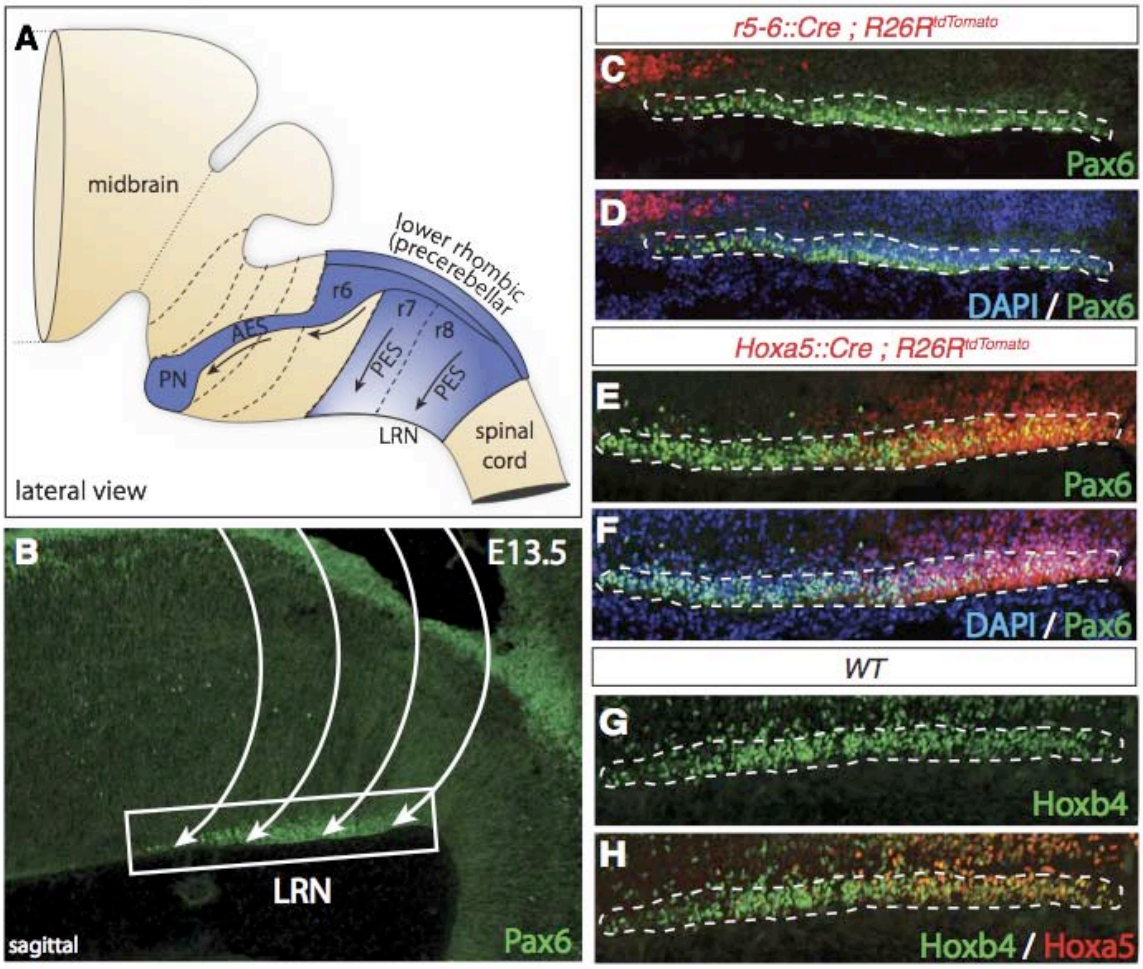

Fig. S10. Topographic organization of migrating lateral reticular nucleus. (**A** to **B**) Lateral reticular nucleus (LRN) neurons originate as the pontine nuclei (PN) from the lower rhombic lip (A) and migrate extramurally to the contralateral side. The migratory stream can be visualized by Pax6 immunostaining on E13.5 sagittal sections (B). (**C** to **D**) Pax6/DAPI double immunohistochemistry on sagittal sections of *r5-6::Cre;R26R*^{tdtomato} embryos at E13.5 showing that LRN neurons lack r5-6 derived progeny. (**E** to **F**) Pax6/DAPI double immunohistochemistry on sagittal sections of *Hoxa5::Cre;R26R*^{tdtomato} embryos at E13.5 showing that posterior LRN neurons are contributed by *Hoxa5::Cre;R26R*^{tdtomato} positive cells. (**G** to **H**) Immunohistochemistry for Hoxb4 (G) and Hoxa5 (H) in migrating LRN neurons on sagittal sections show the posterior restriction of Hoxa5 (H) positive cells. PES: posterior extramural stream; AES: anterior extramural stream.

References

1. A. Lumsden, R. Krumlauf, Patterning the vertebrate neuraxis. *Science* **274**, 1109 (1996).

2. S. Tümpel, L. M. Wiedemann, R. Krumlauf, *Hox* genes and segmentation of the vertebrate hindbrain. *Curr. Top. Dev. Biol.* **88**, 103 (2009).

3. A. F. Farago, R. B. Awatramani, S. M. Dymecki, Assembly of the brainstem cochlear nuclear complex is revealed by intersectional and subtractive genetic fate maps. *Neuron* **50**, 205 (2006).

4. J. Altman, S. A. Bayer, Development of the precerebellar nuclei in the rat: IV. The anterior precerebellar extramural migratory stream and the nucleus reticularis tegmenti pontis and the basal pontine gray. *J. Comp. Neurol.* **257**, 529 (1987).

5. C. I. Rodriguez, S. M. Dymecki, Origin of the precerebellar system. *Neuron* **27**, 475 (2000).

6. M. J. Geisen *et al*., *Hox* paralog group 2 genes control the migration of mouse pontine neurons through slit-robo signaling. *PLoS Biol.* **6**, e142 (2008).

7. K. T. Yee, H. H. Simon, M. Tessier-Lavigne, D. M. O'Leary, Extension of long leading processes and neuronal migration in the mammalian brain directed by the chemoattractant netrin-1. *Neuron* **24**, 607 (1999).

8. S. Nóbrega-Pereira, O. Marín, Transcriptional control of neuronal migration in the developing mouse brain. *Cereb. Cortex* **19**(Suppl. 1), i107 (2009).

9. R. Margueron, D. Reinberg, The Polycomb complex PRC2 and its mark in life. *Nature* **469**, 343 (2011).

<foot>10. Materials and methods are available as supplementary materials on *Science* Online.</foot>

11. E. Bloch-Gallego, F. Ezan, M. Tessier-Lavigne, C. Sotelo, Floor plate and netrin-1 are involved in the migration and survival of inferior olivary neurons. *J. Neurosci.* **19**, 4407 (1999).

12. K. Hong *et al*., A ligand-gated association between cytoplasmic domains of UNC5 and DCC family receptors converts netrin-induced growth cone attraction to repulsion. *Cell* **97**, 927 (1999).

13. D. Kim, S. L. Ackerman, The UNC5C netrin receptor regulates dorsal guidance of mouse hindbrain axons. *J. Neurosci.* **31**, 2167 (2011).

14. X. Lu *et al*., The netrin receptor UNC5B mediates guidance events controlling morphogenesis of the vascular system. *Nature* **432**, 179 (2004).

15. T. B. Leergaard, J. G. Bjaalie, Topography of the complete corticopontine projection: From experiments to principal maps. *Front. Neurosci.* **1**, 211 (2007).

16. P. Rakic, Specification of cerebral cortical areas. *Science* **241**, 170 (1988).

17. M. E. Hatten, Central nervous system neuronal migration. *Annu. Rev. Neurosci.* **22**, 511 (1999).

18. E. C. Lee *et al*., A highly efficient *Escherichia coli*-based chromosome engineering system adapted for recombinogenic targeting and subcloning of BAC DNA. *Genomics* **73**, 56 (2001).

19. T. O. Yau *et al*., Auto/cross-regulation of *Hoxb3* expression in posterior hindbrain and spinal cord. *Dev. Biol.* **252**, 287 (2002).

20. M. Manzanares *et al*., Conserved and distinct roles of *kreisler* in regulation of the paralogous *Hoxa3* and *Hoxb3* genes. *Development* **126**, 759 (1999).

21. A. Gould, N. Itasaki, R. Krumlauf, Initiation of rhombomeric *Hoxb4* expression requires induction by somites and a retinoid pathway. *Neuron* **21**, 39 (1998).

22. P. Soriano, Generalized lacZ expression with the ROSA26 Cre reporter strain. *Nat. Genet.* **21**, 70 (1999).

23. L. Madisen *et al*., A robust and high-throughput Cre reporting and characterization system for the whole mouse brain. *Nat. Neurosci.* **13**, 133 (2010).

24. M. Studer, A. Lumsden, L. Ariza-McNaughton, A. Bradley, R. Krumlauf, Altered segmental identity and abnormal migration of motor neurons in mice lacking *Hoxb-1*. *Nature* **384**, 630 (1996).

25. F. M. Rijli *et al*., A homeotic transformation is generated in the rostral branchial region of the head by disruption of *Hoxa-2*, which acts as a selector gene. *Cell* **75**, 1333 (1993).

26. O. Nyabi *et al*., Efficient mouse transgenesis using Gateway-compatible ROSA26 locus targeting vectors and F1 hybrid ES cells. *Nucleic Acids Res.* **37**, e55 (2009).

27. P. S. Danielian, D. Muccino, D. H. Rowitch, S. K. Michael, A. P. McMahon, Modification of gene activity in mouse embryos in utero by a tamoxifen-inducible form of Cre recombinase. *Curr. Biol.* **8**, 1323 (1998).

28. M. Puschendorf *et al*., PRC1 and Suv39h specify parental asymmetry at constitutive heterochromatin in early mouse embryos. *Nat. Genet.* **40**, 411 (2008).

29. D. C. McIntyre *et al*., Hox patterning of the vertebrate rib cage. *Development* **134**, 2981 (2007).

30. S. L. Ackerman *et al*., The mouse rostral cerebellar malformation gene encodes an UNC-5-like protein. *Nature* **386**, 838 (1997).

31. P. M. Lewis, A. Gritli-Linde, R. Smeyne, A. Kottmann, A. P. McMahon, Sonic hedgehog signaling is required for expansion of granule neuron precursors and patterning of the mouse cerebellum. *Dev. Biol.* **270**, 393 (2004).

32. P. M. Lewis *et al*., Cholesterol modification of sonic hedgehog is required for long-range signaling activity and effective modulation of signaling by Ptc1. *Cell* **105**, 599 (2001).

33. K. Yonehara *et al*., Spatially asymmetric reorganization of inhibition establishes a motion-sensitive circuit. *Nature* **469**, 407 (2011).

34. H. Taniguchi, D. Kawauchi, K. Nishida, F. Murakami, Classic cadherins regulate tangential migration of precerebellar neurons in the caudal hindbrain. *Development* **133**, 1923 (2006).

35. T. Okada, K. Keino-Masu, M. Masu, Migration and nucleogenesis of mouse precerebellar neurons visualized by in utero electroporation of a green fluorescent protein gene. *Neurosci. Res.* **57**, 40 (2007).

36. F. Llambi *et al*., The dependence receptor UNC5H2 mediates apoptosis through DAP-kinase. *EMBO J.* **24**, 1192 (2005).

37. E. D. Leonardo *et al*., Vertebrate homologues of *C. elegans* UNC-5 are candidate netrin receptors. *Nature* **386**, 833 (1997).